JOC Article
pubs.acs.org/joc

Synthesis, Photophysical, and DNA Binding Studies of Fluorescent Tröger's Base Derived 4-Amino-1,8-naphthalimide Supramolecular Clefts

Emma B. Veale* and Thorfinnur Gunnlaugsson*

School of Chemistry, Center for Synthesis and Chemical Biology, Trinity College Dublin, Dublin 2, Ireland

eveale@tcd.ie; gunnlaut@tcd.ie

Received March 31, 2010

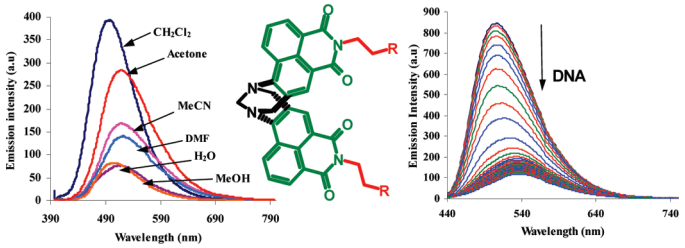

The synthesis and characterization of three bis-1,8-naphthalimide-containing Tröger's bases **1**−**3**, formed from the corresponding 4-amino-1,8-naphthalimide precursors **7**−**9** in a single step, is described. The photophysical investigation of **1**−**3** and **7**−**9** was carried out in various organic solvents as well as in water and as a function of pH using UV/vis and fluorescence spectroscopy. As for their 4-amino-1,8-naphthalimide precursors **7**−**9**, both the ground-state and excited-state characteristics of **1**−**3** were dependent on the polarity and the hydrogen-bonding ability of the solvent medium. The DNA-binding affinities of **1**−**3** were also studied in aqueous solution at pH 7.4, in the presence of *calf-thymus* DNA (*ct*-DNA), using various UV/vis absorption and fluorescence spectroscopic methods. These molecules exhibited significant DNA-binding ability, where large binding values K_b in the range of 10^6 M^{-1} were determined. Such strong binding to *ct*-DNA was maintained even in competitive media (50 and 160 mM NaCl) and was also found to be irreversible regardless of the concentration of the ionic strength. Thermal denaturation experiments also demonstrated that the interaction of **1**−**3** with *ct*-DNA gave rise to significant stabilization in the double-helical structure of DNA. The binding affinity of **1**−**3** for *ct*-DNA was also compared to that of their 4-amino-1,8-naphthalimide precursors **7**−**9**, determined by fitting of data using "intrinsic" methods and ethidium bromide displacement assays. The latter method gives outstanding binding constants for **1**−**3** in the range of 10^7 M^{-1}.

Introduction

The Tröger's base is a well-known chiral cleft-shaped molecule containing a diazocine ring conjugated to two aromatic moieties. The chirality, with a C_2 axis of symmetry, is provided by the presence of the two bridgehead sterogenic nitrogen atoms of the diazocine ring.[1,2] Using X-ray crystal structure analysis, it has been shown that the two aromatic rings are orientated approximately at right angles to each other, with dihedral angles ranging from 90 to 104°, depending on the substituent attached, and thus creating a twist within the molecule. The most common method for the preparation of Tröger's base derivatives has involved treating an aromatic amine with formaldehyde in the presence of an acid, which results in the formation of the desired Tröger's base as a racemic mixture.[2b] The variation in the reaction method has been shown to be quite large, with the possibility of using formaldehyde equivalents such as paraformaldehyde,

(1) (a) Spielman, M. A. *J. Am. Chem. Soc.* **1935**, *57*, 583. (b) Valik, M.; Strongin, R. M.; Král, V. *Supramol. Chem.* **2005**, *17*, 347. (c) Dolensky, B.; Elguero, J.; Kral, V.; Pardo, C.; Valik, M. *Adv. Heterocycl. Chem.* **2007**, *93*, 1. (d) The mechanism for the formation of Tröger's bases has also recently been investigated by: Abella, C. A. M.; Benassi, M.; Santos, L. S.; Eberlin, M. N.; Coelho, F. *J. Org. Chem.* **2007**, *72*, 4048. The mechanism has also been investigated by: (e) Wagner, E. C. *J. Am. Chem. Soc.* **1935**, *57*, 1296. (f) Wagner, E. C. *J. Org. Chem.* **1954**, *19*, 1862. (g) Crossley, M. J.; Try, A. C.; Walton, R. *Tetrahedron Lett.* **1996**, *37*, 6807. (h) Valík, M.; Dolenský, B.; Petříčková, H.; Vašek, P.; Král, V. *Tetrahedron Lett.* **2003**, *44*, 2083. (i) Kobayashi, T.; Moriwaki, T.; Tsubakiyama, M.; Yoshida, S. *J. Chem. Soc., Perkin Trans. 1* **2002**, 1963.

DOI: 10.1021/jo1005697 Published on Web 07/22/2010

hexamethylenetetraamine (HMT),[3] dimethoxymethane,[4] or DMSO[5] and by varying the nature of the acid, where the use of acetic acid, HCl, or trifluoroacetic acid (TFA) have all been reported. Furthermore, many examples of Tröger's base based molecules made from various aromatic moieties, e.g., heterocyclic, naphthalene, phenanthrene, etc., have been reported to date, and often, these possess various additional functional groups where the numbers and the nature of these groups as well as the substitution pattern have been modulated.[6]

The almost perpendicular geometry of the Tröger's base unit has played a considerable role in the field of supramolecular chemistry, specifically within the area of molecular recognition,[1b,c] as well as in the development of "torsion balances", water-soluble cyclophanes, and chiral solvating agents and in the formation of various hydrogen- and metal−ligand-bonding receptors.[7] Recently, the use of these chiral cleft-like molecules has also been preliminarily explored for use in the development of nucleic acid probes.[8] With this in mind, and with the aim of developing novel luminescent and targeting supramolecular structures, we set out to develop Tröger's base derived probes for DNA, formed from the fluorescent 4-amino-1,8-naphthalimide structure,[9a] but prior to our work, Deprez et al.[9b] demonstrated that this fluorescent moiety could be employed in such Tröger's base structures.

The 4-amino-1,8-naphthalimide chromophore has several interesting photophysical properties which are highly desirable for use in supramolecular chemistry[10−14] and caused by the "push−pull" nature of its internal charge transfer (ICT) excited state, arising from the presence of the electron-withdrawing diimide and the electron donating 4-amino moiety. The main advantage for its use, in particular for biological applications, is that the fluorophore absorbs strongly within the visible region and emits at long wavelengths while also possessing good photostability and high quantum yields of emission in varieties of organic and aqueous solvents. In our hands, we have explored the photophysical properties of the 4-amino-1,8-naphthalimide structure in the development of varieties of fluorescent sensors for cations, such as for the sensing of Zn(II) at physiological pH using photoinduced electron transfer (PET) sensors, and in the development of colorimetric sensors for anions in both aqueous and organic media.[10] We have also used this structure for the fluorescence sensing of anions by using charge-neutral urea or thiourea anion-binding receptors,[10b−d] whereby the photophysical properties of the 1,8-naphthalimide chromophore were modulated upon anion recognition regardless of whether the electron-rich thiourea anion receptor was positioned either at the 4-amino position of the aryl ring or at the imide site.[11] Furthermore, we have also investigated the use of 4-amino-1,8-naphthalimide-based PET sensors as novel fluorescent imaging agents of microcracks in bones[14b] and as DNA photocleavage reagents by using 4-nitro- and 4-amino-1,8-naphthalimide-based Ru(II) conjugates;[13] in addition, we, and others, have used the 4-amino-1,8-naphthalimide structure in various supramolecular fields for the detection of organic molecules such as thiols, as DNA targeting molecules, etc.[14]

In this paper, we discuss the synthesis and the characterization of three 4-amino-1,8-naphthalimide-based Tröger's bases **1**−**3**, formed from their corresponding 4-amino-1,8-naphthalimide analogues, and an evaluation of their various

(2) (a) Wilcox, C. S. *Tetrahedron Lett*. **1985**, *26*, 5749. (b) Sucholeiki, I.; Lynch, V.; Phan, L.; Wilcox, C. S. *J. Org. Chem*. **1988**, *53*, 98. (c) Maitra, U.; Bag, B. G.; Rao, P.; Powell, D. *J. Chem. Soc., Perkin Trans. 1* **1995**, 2049. (d) Crossley, M. J.; Hambley, T. W.; MacKay, L. G.; Try, A. C.; Walton, R. *J. Chem. Soc., Chem. Commun*. **1995**, 1077. (e) Cudero, J.; Pardo, C.; Ramos, M.; Gutierrex-Puebla, E.; Monge, A.; Elguero, J. *Tetrahedron* **1997**, *53*, 2233. (f) Brotherhood, P. R.; Luck, I. J.; Blake, I. M.; Jensen, P.; Turner, P.; Crossley, M. J. *Chem.—Eur. J*. **2008**, *14*, 10967. (g) Weilandt, T.; Kiehne, U.; Schnakenburg, G.; Lutzen, A. *Chem. Commun*. **2009**, 2320. (h) Kiehne, U.; Bruhn, T.; Schnakenburg, G.; Frohlich, R.; Bringmann, G.; Lutzen, A. *Chem.—Eur. J*. **2008**, *14*, 4246. (i) Michon, C.; Sharma, A.; Bernardinelli, G.; Francotte, E.; Lacour, J. *Chem. Commun*. **2010**, *46*, 2206. (j) Weilandt, T.; Kiehne, U.; Bunzen, J.; Schnakenburg, G.; Lutzen, A. *Chem.—Eur. J*. **2010**, *16*, 2418. (k) Du, X.; Sun, Y. L.; Tan, B. E.; Teng, Q. F.; Yao, X. J.; Su, C. Y.; Wang, W. *Chem. Commun*. **2010**, *46*, 970. (l) Dalla Favera, N.; Kiehne, U.; Bunzen, J.; Hytteballe, S.; Lutzen, A.; Piguet, C. *Angew. Chem., Int. Ed*. **2010**, *49*, 125.

(3) (a) Webb, T. H.; Suh, H.; Wilcox, C. S. *J. Am. Chem. Soc*. **1991**, *113*, 8554. (b) Johnson, R. A.; Gorman, R. R.; Wnuk, R. J.; Crittenden, N. J.; Aiken, J. W. *J. Med. Chem*. **1993**, *36*, 3202.

(4) Bag, B. G.; Maitra, U. *Synth. Commun*. **1995**, *25*, 1849.

(5) Li, Z.; Xu, X; Peng, Y.; Jiang, Z.; Ding, C.; Qian, X. *Synthesis* **2005**, *8*, 1228.

(6) (a) Jensen, J.; Wärnmark, K. *Synthesis* **2001**, *12*, 1873. (b) Hansson, A. P.; Jensen, J.; Wendt, O. F.; Wárnmark, K. *Eur. J. Org. Chem*. **2003**, 3179. (c) Bhuiyan, M. D. H.; Mahon, A. B.; Jensen, P.; Clegg, J. K.; Try, A. C. *Eur. J. Org. Chem*. **2009**, 697. (d) Valík, M.; Čejka, J.; Havlík, M.; Král, V.; Dolensky, B. *Chem. Commun* **2007**, 3835. (e) Artacho, J.; Nilsson, P.; Bergquist, K.-E.; Wendt, O. F.; Wärnmark, K. *Chem.—Eur. J*. **2006**, *12*, 2692. (f) Hansson, A.; Wixie, T.; Bergquist, K.-E.; Wärnmark, K. *Org. Lett*. **2005**, *7*, 2019.

(7) (a) Paliwal, S.; Geib, S.; Wilcox, C, S. *J. Am. Chem. Soc*. **1994**, *116*, 4497. (b) Wilcox, C. S.; Greer, L. M.; Lynch, V. *J. Am. Chem. Soc*. **1987**, *109*, 1865. (c) Wilen, S. H.; Qi, J, Z.; Williard, P. G. *J. Org. Chem*. **1991**, *56*, 485. (d) Reek, J. N. H.; Schenning, A. P. H. J.; Bosman, A. W.; Meijer, E. W.; Crossley, M. J. *Chem. Commun*. **1998**, 11. (e) Hansson, A. P.; Norrby, P.-O.; Wärnmark, K. *Tetrahedron Lett*. **1998**, *39*, 4565. (f) Miyake, M.; Wilcox, C. S. *Heterocycles* **2002**, *56*, 515.

(8) (a) Yashima, E.; Akashi, M.; Miyauchi, N. *Chem. Lett*. **1991**, 1017. (b) Tatibouet, A.; Demeunynck, M.; Andraud, C.; Collet, A.; Lhomme, J. *Chem. Commun*. **1999**, 161. (c) Bailly, C.; Laine, W.; Demeunynck, M.; Lhomme, J. *Biophys. Res. Commun*. **2000**, *273*, 681. (d) Baldeyrou, B.; Tardy, C.; Bailly, C.; Colson, P.; Houssier, C.; Charmantray, F.; Demeunynck, M. *Eur. J. Med. Chem*. **2002**, *37*, 315. (e) Valík, M.; Malina, J.; Palivec, L.; Foltýnová, J.; Tkadlecová, M.; Urbanová, M.; Brabec, V.; Král, V. *Tetrahedron* **2006**, *62*, 8591.

(9) (a) Veale, E. B.; Frimannsson, D. O.; Lawler, M.; Gunnlaugsson, T. *Org. Lett*. **2009**, *11*, 4040. (b) Deprez, N. R.; McNitt, K. A.; Petersen, M. E.; Brown, R. G.; Lewis, D. E. *Tetrahedron Lett*. **2005**, *46*, 2149.

(10) (a) Parkesh, R.; Lee, T. C.; Gunnlaugsson, T. *Org. Biol. Mol. Chem*. **2007**, *5*, 310. (b) Gunnlaugsson, T.; Lee, T. C.; Parkesh, R. *Org. Biomol. Chem*. **2003**, *1*, 3265. (c) Gunnlaugsson, T.; Glynn, M.; Tocci, G. M.; Kruger, P. E.; Pfeffer, F. M. *Coord. Chem. Rev*. **2006**, *250*, 3094. (d) Ali, H. D. P.; Kruger, P. E.; Gunnlaugsson, T. *New J. Chem*. **2008**, *32*, 1153. (e) Duke, R. M.; Gunnlaugsson, T. *Tetrahedron Lett*. **2007**, *48*, 8043. (f) Elmes, R. B. P.; Gunnlaugsson, T. *Tetrahedron Lett*. **2010**, *51*, 4082.

(11) (a) Veale, E. B.; Tocci, G. M.; Pfeffer, F. M.; Kruger, P. E.; Gunnlaugsson, T. *Org. Biomol. Chem*. **2009**, *7*, 3447. (b) Veale, E. B.; Gunnlaugsson, T. *J. Org. Chem*. **2008**, *73*, 8073.

(12) (a) Lowe, A. J.; Pfeffer, F. M. *Chem. Commun*. **2008**, 1871. (b) Pfeffer, F. M.; Seter, M.; Lewcenko, N.; Barnett, N. W. *Tetrahedron Lett*. **2006**, *47*, 5251. (c) Pfeffer, F. M.; Buschgens, A. M.; Barnett, N. W.; Gunnlaugsson, T.; Kruger, P. E. *Tetrahedron Lett*. **2005**, *46*, 6579. (d) Li, Y.; Cao, L. F.; Tian, H. *J. Org. Chem*. **2006**, *71*, 8279. (j) Xu, S.; Chen, K. C.; Tian, H. *J. Mater. Chem*. **2005**, *15*, 2676. (e) Gunnlaugsson, T.; McCoy, C. P.; Morrow, R. J.; Phelan, C.; Stomeo, F. *ARKIVOC* **2003**, *8*, 216. (f) He, H.; Mortellaro, M. A.; Leiner, M. J. P.; Fraatz, R. J.; Tusa, J. K. *J. Am. Chem. Soc*. **2003**, *125*, 1468. (g) de Silva, A. P.; Gunaratne, H. Q. N.; Gunnlaugsson, T. *Tetrahedron Lett*. **1998**, *39*, 5077. (h) Lowe, A. J.; Dyson, G. A.; Pfeffer, F. M. *Eur. J. Org. Chem*. **2008**, 1559. (i) Gunnlaugsson, T.; Kruger, P. E.; Lee, T. C.; Parkesh, R.; Pfeffer, F. M.; Hussey, G. M. *Tetrahedron Lett*. **2003**, *44*, 6575.

(13) Ryan, G. J.; Quinn, S.; Gunnlaugsson, T. *Inorg. Chem*. **2008**, *47*, 401.

(14) (a) Chen, Z.; Liang, X.; Zhang, H.; Xie, H.; Liu, J.; Xu, Y.; Zhu, W.; Wang, Y.; Wang, X.; Tan, S.; Kuang, D.; Qian, X. *J. Med. Chem*. **2010**, *53*, 2589. (b) Parkesh, R.; Lee, T. C.; Gunnlaugsson, T. *Tetrahedron Lett*. **2009**, *50*, 4114. (c) Xu, Z.; Xiao, Y.; Qian, X.; Cui, J.; Cui, J. *Org. Lett*. **2005**, *7*, 889. (d) Guo, X.; Qian, X.; Jia, L. *J. Am. Chem. Soc*. **2004**, *126*, 2272. (e) de Silva, A. P.; Gunaratne, H. Q. N.; Gunnlaugsson, T. *Tetrahedron Lett*. **1998**, *39*, 5077. (f) Aveline, B. M.; Matsugo, S.; Redmond, R. W. *J. Am. Chem. Soc*. **1997**, *119*, 11785. (g) Saito, I.; Takayama, M.; Kawanishi, S. *J. Am. Chem. Soc*. **1995**, *117*, 5590.

SCHEME 1. Synthesis of 1,8-Naphthalimide-Based Tröger's Bases 1−3

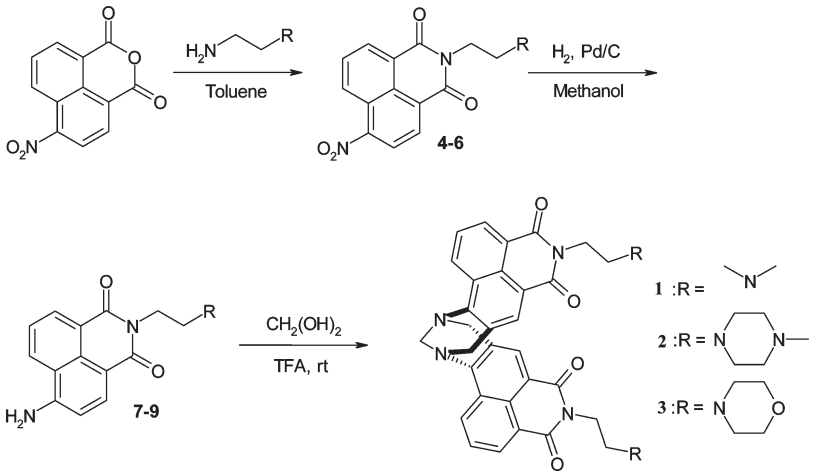

photophysical properties of these systems in both organic solvents and in water, and as a function of pH using UV/vis absorption and fluorescence excitation and emission spectroscopy. We then utilized the results from such studies as a basis for investigating their interaction with DNA using the same spectroscopic techniques while also carrying out ethidium bromide displacement assays and thermal denaturation measurements.

Results and Discussion

Synthesis of 1−3. The three-step synthesis of **1**−**3** is shown in Scheme 1. Treating 4-nitro-1,8-naphthalic anhydride with the relevant alkylamine and refluxing the two components in anhydrous toluene for 24 h gave rise to the formation of the desired 4-nitro-1,8-naphthalimide precursors **4**−**6** (see the Supporting Information for the ^{1}H and ^{13}C NMR spectra of **5** and **6**) in ca. 80% yield after a recrystallization from ethanol. Subsequent reductions by catalytic hydrogenation with 10% Pd/C, at 3 atm of H_2, in methanol gave the corresponding amino derivatives **7**−**9** in good yields (see the Supporting Information for the ^{1}H and ^{13}C NMR of **8** and **9**). Formation of **1**−**3**, as racemic mixtures, was initially attempted by treating the precursors **7**−**9** with an ice-cold mixture of 7 equiv of formaldehyde and concentrated HCl in ethanol and stirring the resulting mixture at 60 °C for 72 h. On all occasions, this led to the isolation of **1**−**3** as pure compounds but in rather poor yields (ca. < 30%) after basic workup and purification using column chromatography on flash silica (CH_2Cl_2/MeOH−NH_3, 95:5). As a means of optimizing the reaction conditions, **7**−**9** were also treated with 1.5 equiv of formaldehyde in neat TFA over 12 h at room temperature. This led to the formation of **1**−**3** after basic workup and extraction with CH_2Cl_2 in much improved yields of ca. 60% after recrystallization from ethanol. The ^{1}H NMR spectra ($CDCl_3$, 400 MHz) of **1** (see the Supporting Information for all ^{1}H and ^{13}C NMR spectra of **1**−**3**) confirmed its identity by the presence of well-separated doublet of doublets between ca. 5.14 and 4.34 ppm, pertaining to the methylene protons of the diazocine ring, while also clearly reflecting the C_2 plane of symmetry of the molecules. All of the signal resonances were assigned by ^{1}H−^{1}H-COSY and HMQC experiments (see the Supporting Information), and all new compounds were fully characterized using standard techniques.

Spectroscopic Evaluation in Solvents of Varying Polarity. The absorption and the fluorescence emission spectra of the 4-amino-1,8-naphthalimide derivatives are generally both solvent as well as temperature dependent. The reason for this is that their internal charge-transfer excited state (ICT) gives rise to a large excited-state dipole moment, which can be stabilized or destabilized depending on the solvent's polarity.[15] Hence, properties such as fluorescent emission wavelength, lifetime, and quantum yield (Φ_{FI}) have all been found to be dependent on these solvents and their hydrogen-bond donor (HBD) or acceptor (HBA) capacity.[15] As a means of investigating whether the ICT excited state of **1**−**3** was also solvochomomic, the absorption and the fluorescence emission and excitation spectra of **1**−**3** were recorded in protic and aprotic solvents of varying polarity (Figure S8, Supporting Information).

The absorption spectra of **1**−**3** were indeed found to be highly solvent dependent, whereby Figure S8 (Supporting Information) shows the various absorption spectra observed for **2** in different solvents, indicating that the ground state of these Tröger's bases was most stabilized in polar protic solvents and in a manner similar to that observed for the precursor **7**. The results from this investigation are summarized in Table S1 (Supporting Information). As an example, in methanol, the absorption spectra of **2** showed a broad band between 280 and 450 nm, with λ_{max} at 385 nm (ε = 11452 mol^{-1} dm^3 cm^{-1}) and a second more structural band centered at 230 nm. This band was, however, slightly blue-shifted in comparison to the precursor **7** when recorded in methanol. This is most likely due to a lack of ability of the lone pairs of the 4-amino moiety of the diazocine ring moiety to participate as strongly in the "push−pull" nature of the ICT excited state of the naphthalimide moiety of **2** in comparison that that of the 4-amino moiety in **6**, which is not conformationally restricted.[15] Nevertheless, as demonstrated in Figure S8a (Supporting Information), the absorption spectra of **2** were on all occasions affected by the polarity and or the HBA of the medium, and the same solvent dependence was observed for **2** as had been established for **7**. This

(15) (a) Kucheryavy, P.; Li, G.; Vyas, S.; Hadad, C.; Glusac, K. D. *J. Phys. Chem. A* **2009**, *113*, 6453. (b) Saha, S.; Samanta, A. *J. Phys. Chem. A* **2002**, *106*, 4763. (c) Loving, G. S.; Imperiali, B. *Biocong. Chem.* **2009**, *20*, 2133.

suggests that **2** also possess an ICT character. Consequently, the influences of solvent polarity on the photophysical behavior of **1**−**3** were further studied using both fluorescence emission and excitation spectroscopy. Table S1 (Supporting Information) summarizes the results from the emission studies, which also confirmed the ICT nature of the excited state. Upon excitation of **2** in CH_2Cl_2 at λ_{max} 385 nm, the resulting emission spectrum exhibited a broad emission band centered at 497 nm Figure S8b (Supporting Information), which exhibited significant bathochromic shifts and a decrease in the emission intensity upon an increase in the polarity and HBD ability of the solvent. This effect was more pronounced than that seen in the absorption maximum of **1**−**3**, indicting that the solvent stabilization was greater in the excited state of **2**. Such stabilization has previously been shown to occur for naphthalimide-based ICT fluorophores.[15] The decrease in the emission intensity of **1**−**3** as a function of increasing solvent polarity was also accompanied by a reduction in their fluorescence quantum efficiencies, as shown in Table S1 (Supporting Information) for **2**. Such an effect has been previously reported and is in agreement with the low fluorescent quantum efficiencies of *N*-substituted 4-amino-1,8-naphthalimide derivatives.[16] Hence, the 4-amino-1,8-naphthalimide-based Tröger's bases **1**−**3** can be described as possessing an ICT excited state as their synthetic precursors.[15] Moreover, given the fact that the fluorescence emission of **1**−**3** is highly dependent on solvent polarity, we foresaw that, upon binding of these structures to DNA, significant changes would be expected to be observed in their emission spectra as a function of increasing DNA concentration, particularly if these structures functioned as DNA intercalators.

Investigating the Photophysical Properties of 1−3 and 7−9 as a Function of pH. With the aim of developing naphthalimide-based Tröger's bases as highly efficient DNA targeting agents, **1**−**3** were functionalized with a dialkylamino moiety at the side chains of the 1,8-naphthalimide structure. The objective was that these tertiary amines should, upon protonation at physiological pH, make **1**−**3** substantially soluble in aqueous buffered solution, while the resulting dicationic product would further enable the electrostatic interaction of these structures with the negatively charged phosphate backbone of the DNA helix. Given the almost orthogonal nature of the two naphthalimides within the Tröger's base structures **1**−**3**, it was anticipated that these would bind to DNA, possibly by a dual action, where one of these naphthalimide units would be able to intercalate within the double stranded DNA structure, while the second one would most likely give rise to groove binding. However, we also foresaw that the dominant DNA binding mode would be via groove binding alone. This protonation would also possibly affect the photophysical properties of these systems, which needed to be investigated.

4-Amino-1,8-naphthalimide structures, possessing an electron-rich moiety conjugated via a spacer, at either the 4-amino moiety or the imine moiety have been reported to participate in excited-state quenching of the naphthalimide via a PET mechanism from the electron-rich moiety.[10] While this quenching is particularly efficient for systems that have such quenchers conjugated via the 4-amino moiety, those possessing the quenching moiety at the imide side, such as the precursors **7**−**9**, normally do not give rise to significant changes in their emission spectra as a function of pH.[17] This phenomenon has been referred to as *directional PET quenching* and has been investigated by both de Silva et al.[17a] and Macrus et al.,[17b] who proposed that the directionality occurred "due to the difference in the electronic coupling matrix elements (jVj) for the two reactions". Because of this, the PET quenching from the 4-amino side has been estimated to be ca. $\sim 10^4$ times faster than from the imide side. Hence, we anticipated that the nature of the ground and the excited state of **1**−**3** would follow this trend and be pH independent. This is important as it would exclude any "false-positive" pH-dependent response from such systems upon binding to DNA.

To confirm this, the pH dependence of the 4-amino-1,8-naphthalimide precursors **7**−**9** was first investigated as a function of pH in water using 100 mM NaCl to maintain a constant ionic strength. In general, and as expected, only minor changes were observed in both the absorption and the emission spectra of these compounds as a function of pH, as demonstrated for **7** (see various parameters in Table S2 data for **8** and **9**, Supporting Information). Here, the absorption spectra of **7**, consisting of a main ICT band centered at 450 nm, can be considered to be independent of pH, with only minor changes occurring at higher energy upon titrating an acidic solution of **7** with base. Similarly, the fluorescence emission of **7** was only effected marginally by pH, being ca. 8% enhanced, which indicates that only a minor PET quenching is operating from the terminal amine, which upon protonation is blocked, due to an increased oxidation potential of the resulting ammonium species, with a subsequent, although minor, enhancement in the fluorescence of **7**. Having confirmed the expected pH independence of **7**−**9**, we next investigated the pH dependence for **1**−**3** (see Table S2, Supporting Information, for various parameters). Similar to that observed in for **7**−**9**, only minor changes were seen in the fluorescence emission spectra of **1**−**3** as a function of pH, as demonstrated for **1** in Figure 1b (see the Supporting Information for **2** and **3**). However, unlike that seen above for **7**, where the emission was slightly enhanced, the emission of **1** was quenched by ca. 10%. Similar results were observed for **2** and **3**, where a marginally larger quenching of ca. 30 and 15% was observed for **2** and **3**, respectively (see the Supporting Information).

The normalized changes observed in the ICT emission (λ_{max}) of **1** and **7** are plotted in Figure S9b (Supporting Information) and clearly demonstrate that both are affected within the same pH window, which in fact corresponds to the expected pK_a of the terminal tertiary amine.[17a] Hence, the quenching of the ICT states in both of these structures has to be associated with the terminal amines. However, one would have expected to observe fluorescence enhancement due to blocking of PET upon protonation of the terminal amine, and that is clearly not observed here. Nevertheless, from these changes, we were able to estimate the pK_a to be ca. 8.7,

(16) (a) Noukakis, N.; Suppan, P. *J. Lumin.* **1991**, *47*, 285. (b) Pardo, A.; Poyato, J. M. L.; Martin, E.; Camacho, J. J.; Reyman, D. *J. Lumin.* **1990**, *46*, 381.

(17) (a) de Silva, A. P.; Rice, T. E. *Chem. Commun.* **1996**, 163. (b) See also: de Silva, A. P.; Goligher, A.; Gunaratne, H. Q. N.; Rice, T. E. *ARKIVOC* **2003**, *7*, 229. (c) Gao, Y. Q.; Marcus, R. A. *J. Phys. Chem. A* **2002**, *106*, 1956. (d) Xiao, Y.; Fu, M.; Qian, X.; Cui, J. *Tetrahedron Lett.* **2005**, *46*, 6289. (e) Tian, H.; Xu, T.; Zhao, Y.; Chen, K. *J. Chem. Soc., Perkin Trans. 2* **1999**, 545. (f) Wanga, J.; Qian, X. *Chem. Commun.* **2006**, 109.

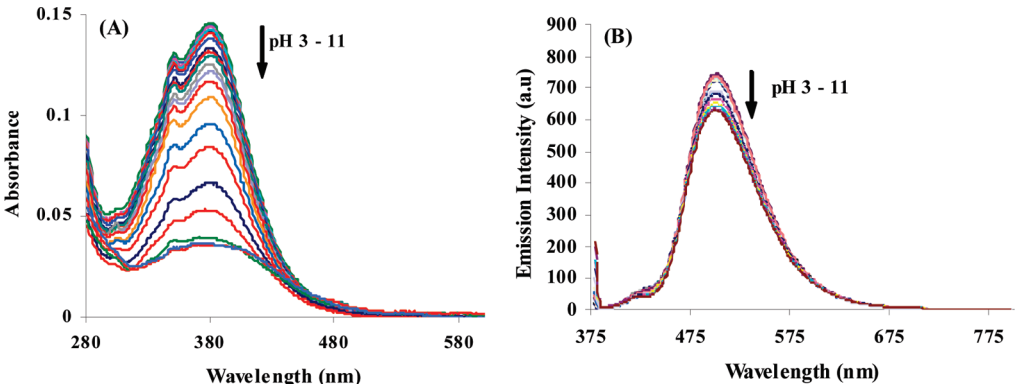

FIGURE 1. Absorption (A) and the emission (B) spectra of **1** (11 μM) upon a gradual increase in pH.

Table S2 (see the Supporting Information) by fitting the data to $pK_a(S_1) = pH - \log(I_{fAH} - I_{fA})/(I_{fA} - I_{fA^-})$, where I_{fAH} and $I_{fA}-$ are the emission intensities in acidic and basic solution and I_{fA} is the emission intensity at each of the pH values),[17a] which is similar to that observed for **7** and, hence, would correspond to the protonation of the terminal amino moiety and not due to the protonation of the amino moieties of the diazocine ring. Likewise, for **2** and **3**, pK_a's of ca. 8.2 and 6.0, respectively, Table S2 (Supporting Information), were estimated from the changes in the ICT band of their respective emissions, and both are in good agreement with that observed for fitting the changes seen in the emission spectra of **8** and **9**, respectively. With the view of further explaining this difference between the emission changes observed in **1**−**3** vs that of **7**−**9**, we investigated the changes in the absorption spectra of **1**−**3**.

As discussed above, we did not anticipate observing any significant changes in the absorption spectra of the ICT bands of **1**−**3** as a function of pH, due to the presence of the *fluorophore*−*spacer*−*receptor* structures. However, unlike that observed for **7**−**9**, the Tröger's bases **1**−**3** all displayed significant changes in their absorption spectra as a function of pH. The changes observed in the absorption spectra of **1**, as a function of pH, are shown in Figure 1a, and clearly demonstrate that upon addition of base the ICT band centered at 380 nm decreased by ca. 70%. Furthermore, these changes were found to be fully reversible as upon acidification the original spectrum was reinstated in alkaline media. These pH-dependent changes observed in the absorption spectra of **1** also help in explaining why the emission of **1** is quenched upon protonation of the amine, as one could envisage that the naphthalimide excited state is less populated and, hence, less emissive. However, PET should also be blocked in acidic media and, hence, in some way compensates for the diminished emission.

The changes in the absorption spectra of **1** for the ICT band are shown in Figure S9a (see the Supporting Information) where the normalized changes observed for the ICT band of **1** are compared to that observed for the corresponding precursor **7**. Comparing these results to that shown in Figure S9b (Supporting Information), for the changes in the emission spectra of **1**, it becomes clear that the changes in the absorption spectra occurs within the pH window for both the ground and the excited state; and hence, demonstrate that these are associated with the protonation of the terminal amine. Analysis of the changes in the absorption spectra (by fitting it to $pK_a(S_o) = pH - \log(Abs_{AH} - Abs_A)/(Abs_A - Abs_{A^-})$, where Abs_{AH} and $Abs_A{}^-$ are the absorbance values in acidic and basic solution and Abs_A is the absorbance value at each pH value)[17a] gave a pK_a of 7.7, which we assign to the ground-state pK_a of the terminal amine in **1**.

Similarly, analysis of the changes in the absorption spectra of **2** and **3** as a function of pH showed that these changes occurred with the same pH window as seen in the emission spectra of **2** and **3**, respectively, Table 2S (Supporting Information). When recorded in acidic solution, both gave rise to similar absorbance spectra, which exhibited a broad band centered at 381 nm and a sharp band at 232 nm, like that seen for **1**. Upon titration with base, the absorption spectrum of **2** was found to decrease by 40%, whereas the absorbance band of **3** decreased by 80%. As seen above, these changes were found to be fully reversible, and from these changes, pK_a of 8.0 ($\pm$0.1) and 6.22 ($\pm$0.1) were determined for **2** and **3**, respectively.

It is clear from these investigations that while the precursors **7**−**9** obey typical PET behavior (as is to be expected for such structures), the changes observed in the ground and the excited states of **1**−**3** are quite different, while at the same time, similar pK_a's can be determined from such changes for the two familes of structures, all of which were assigned to the protonations of their respective terminal amines. The changes in the absorption spectra clearly suggest that there is significant pH dependence in the ground state of **1**−**3**, which, on the basis of a determination of the pK_a values from these change, we assign to an interaction between the naphthalimide unit and the terminal amines of these structures, which is absent in **7**−**9**. It is also worth pointing out the absence of any exciplex emission from these structures; which indicate that this is not an excited state phenomenon. However, some changes were observed in the λ_{max} of the emission of **1**−**3**, as a function of pH, Table 2S (Supporting Information), where the emission is red-shifted in alkaline media compared to that in acidic media. However, as we do observed PET quenching for the precursors, we cannot exclude that the protonation of the terminal amine in **1**−**3** also prevents, or reduces, any PET quenching in **1**−**3**. While normally this (as was seen for **7**−**9**) would give rise to a fluorescence enhancement associated in the emission of such systems, then the fact that the absorption spectra is greatly affected by pH might be overshadowing this affect, as the excited states of **1**−**3** is less populated in acidic media than in alkaline solution.

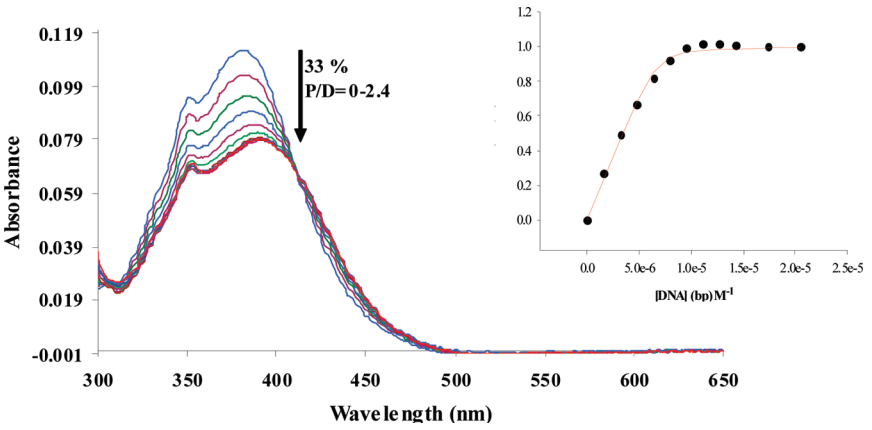

FIGURE 2. Absorbance spectrum of **1** (8.7 μM) in 10 mM phosphate buffer (pH 7.4) with increasing concentration of *ct*-DNA. Inset: Plot of $(\varepsilon_a - \varepsilon_f)/(\varepsilon_b - \varepsilon_f)$ vs DNA (M^{-1}, bp) (●) and the best fit of the data (−) using the Bard model.

From these accumulative results, we can conclude that the presence of the diazocine ring in **1**−**3** enables significant ground-state interactions to take place between the naphthalimide fluorophores and their respective terminal amines. This is most likely due to an enhanced contact between the two parts which is caused by presence of the Tröger's base moiety (e.g., the two fluorophores become almost orthogonal to each other). However, while this interaction is highly pronounced in the ground state of **1**−**3**, the corresponding changes in the emission spectra are small in comparison, and most likely due to a combination of two processes; the blocking of PET upon protonation of the terminal amine, and a reduced population of the excited states of **1**−**3** in acidic media. Having investigated the pH dependence on both the ground and the excited states of **1**−**3** and **7**−**9**, we next investigated the ability of these structures to bind to DNA.

Spectroscopic DNA Binding Evaluations of 1−3 and 7−8. Absorption Studies. The Tröger's bases **1**−**3** were designed as potential C_2-symmetrical-based DNA-binding molecules possessing tertiary amino functionalities at the "terminus" of their side chains, which would render them water-soluble while also providing favorable electrostatic interactions with the negatively charged backbone of DNA under physiological pH conditions. From the results of the previous section, we showed that both **1** and **2** would be fully or partially protonated and, consequently, would be expected to have high electrostatic affinity for the phosphate backbone of DNA (in comparison to **3**, which has a lower pK_a of ca. 6.2) within the physiological pH window. Furthermore, it was anticipated that the cleftlike structure of the Tröger's base moiety would give rise to an orthogonal shape to the naphthalimide chromophores, which would perhaps assist in their binding with DNA either by an intercalation mechanism or by sitting within either the minor or major grooves of the DNA structure.

The ground-state and excited-state investigations of **1**−**3** with *ct*-DNA were carried out in aqueous 10 mM phosphate buffer solution at pH 7.4 in the presence of 0, 50, and 160 mM NaCl concentrations. The DNA binding affinity of **3**, having a pK_a of ca. 6.2, was also analyzed in 10 mM Coadylate buffer at pH 6.0. The absorbance spectra for **1**−**3** were all considerably affected upon binding to *ct*-DNA, as shown in Figure 2 for **1** in 10 mM phosphate buffer at pH 7.4, whereby the addition of *ct*-DNA (0 → 21 μM) resulted in a significant hypochromism of 33% at the λ_{max}(381 nm), with an accompanying bathochromic shift of 11 nm and a clear isosbestic point at 415 nm, all of which occurred up to a P/D (phosphate/dye ratio) of <1. However, upon a further addition of *ct*-DNA within the 23−172 μM concentration range, the absorbance spectrum of **1** exhibited a small enhancement of 18% at λ_{abs} 392 nm. Thereafter, no changes were observed. This is perhaps indicative of a second mode of binding which takes place after initial binding, but such a phenomenon has also been reported by Kelly et al. for the binding of methylene blue to DNA.[18] These results are summarized in Table 1.

TABLE 1. Photophysical Properties of 1−3 (10 mM Phosphate Buffer, pH 7.4) in the Presence of *ct*-DNA

property	**1**	**2**	**3**	**3**[k]
λ_{maxF}[a] (nm)	381	381	391	385
λ_{maxB}[b] (nm)	392	392	391	385
B_{shift}[c] (nm)	11	11	0	0
ε_F[d] (M^{-1} dm^3 cm^{-1})	12893	11452	10220	10220
ε_B[e] (M^{-1} dm^3 cm^{-1})	7909	6959	6708	7518
% Hypo[f]	33	36	31	25
IP[g] (nm)	415	415		
bound P/D[h]	1.3 → 2.4	1.3 → 2.4	5 → 12	2.3 → 7
% Hyper[i]	18	25	10	16
bound P/D[j]	23	20	25	22

[a] λ_{maxF} is the wavelength of maximum absorbance of the free compound (P/D = 0). [b] λ_{maxB} is the wavelength of maximum absorbance of the compound bound to *ct*-DNA (P/D = 1.3−5). [c] B_{shift} is the bathochromic shift observed in λ_{max} from the free to the bound compound. [d] ε_F is the extinction coefficient of the free compound. [e] ε_B is the extinction coefficient of compound bound to *ct*-DNA at λ_{max} Abs. Plotting 1/[DNA] vs λ_{max} and dividing the *y*-intercept by [Dye (P/D = 0)] gives ε_B [f] % Hypo is the percentage hypochromicity at λ_{max} Abs (P/D = 0). [g] IP is the isosbestic point for titration of the compound with *ct*-DNA. [h] Bound P/D values are calculated in base pairs and correlate to the phosphate to dye ratio at which the decrease in the absorbance spectra reach an initial plateau. [i] % Hyper is the percentage hyperchromicity at λ_{max} Abs that occurs after the plateau of the initial hypochromic effect. [j] Bound P/D at which the subsequent increase in the absorbance spectra reach a plateau. Errors: λ_{max} ± 0.2 nm, ε ± 100. [k] Troger's base **3** (coadcylate buffer, pH 6.0).

Upon binding to *ct*-DNA at low ionic strength, 50 mM NaCl, the changes observed in the absorption spectra of **1** were analogous to those in the absence of added salt and even

(18) Tuite, E.; Kelly, J. M. *Biopolymers* **1995**, *35*, 419.

TABLE 2. Binding Constants Determined from Changes in the Absorbance Spectra for 1−3 in 10 mM Phosphate Buffer at pH 7.4 and in the Presence of Competitive Media and 3* in 10 mM Codaylate Buffer at pH 6.0

K_b ($\times 10^6$ M^{-1})	1	2	3	3*
0 mM NaCl	7.40 (±0.2)	4.24 (±0.3)	0.78 (±0.2)	2.26 (±0.09)
50 mM NaCl	3.00 (±0.3)	2.70 (±0.07)		
160 mM NaCl	0.61 (±0.31)	0.50 (±0.1)		

at higher 160 mM NaCl ionic strength, and the degree of hypochromism was only slightly smaller at 26% with such changes reaching a plateau at a P/D ratio of ca. 6 (see the Supporting Information for the binding curve of **1**).

By analyzing the changes in the absorbance spectra by using the Bard model[19] (see the Supporting Information), large binding constants, K_b, for **1**−**3** were determined, Table 3. In the absence of NaCl salt, large K_b values of 7.40 (±0.2) × 10^6 M^{-1} and 4.24 (±0.3) × 10^6 M^{-1} were determined for **1** (see fitting to the Bard plot as an inset in Figure S10 in the Supporting Information) and **2**, respectively, which is of similar size magnitude to that often observed for DNA binding molecules consisting of many Ru(II) polypyridyl derived complexes.[13] Furthermore, in more competitive media, such as in the presence of 160 mM NaCl, these binding constants still remained within the range of 10^6 M^{-1}, clearly demonstrating that these compounds have a high affinity for DNA, even in highly competitive media. As shown in Table 2, a good correlation between K_b and pK_a values were upheld for **1**−**3** with the trends in binding affinity being in the range **1** > **2** > **3**. Furthermore, the binding affinity of **3**, when measured in 10 mM Coadylate buffer at pH 6, was determined to be significantly higher, with a K_b = 2.26 (±0.09) × 10^6 M^{-1} compared to that determined at pH 7.4, K_b = 0.78 (±0.2) × 10^6 M^{-1}. This again reflects the effect of pK_a of the terminal side chains with the strength of DNA binding for **1**−**3**.

The DNA binding of **7** and **8** were also investigated in a manner analogous to that described above. The absorption spectrum of **7** (8.7 μM) in 10 mM phosphate buffer (pH 7.4) is shown in Figure S10 (Supporting Information). Upon increasing the concentration of *ct*-DNA (0−245 μM), the absorption band centered at 433 nm was hypochromially shifted by ca. 42%, along with a bathochromic shift of 11 nm. The appearance of an unclear "isosbestic point" ranging between 471 and 475 nm was also observed. Nevertheless, the significant decrease and the red shift in absorbance indicates that **7** has significant binding affinity for *ct*-DNA. However, the biphasic DNA binding exhibited by **1** was not evident for **7**. Such a result is quite interesting and clearly highlights the difference in the ground-state interactions of **1** vs **7** upon binding to DNA. Similar decreases in the absorption spectra have been observed for unsubstituted[20,21] and 3- and 4-amino-substituted 1,8-naphthlaimides.[22,23] Therefore, the presence of the Tröger's base moiety is obviously influencing the manner in which the naphthalimide chromophore interacts with DNA. Similar changes were also seen for **8** (8.7 μM, 10 mM phosphate buffer, pH 7.4), where the absorption spectra exhibited a hypochromic effect of 36% at λ_{max} 433 nm upon binding to *ct*-DNA. The binding constants for **7** and **8** were determined according to the Bard model[19] and were found to be K_b = 2.8 (±0.05) × 10^6 M^{-1} and 1.44 (±0.4) × 10^6 M^{-1}, for **7** and **8**, respectively. This was expected because molecules which contain the 1,8-naphthalimide structure have been well characterized as a strong DNA binding agents.[24] Nevertheless, the binding constants for both **7** and **8** are about three times smaller in magnitude than that determined for **1** and **2**, thus clearly demonstrating that the Tröger's base moiety significantly enhances the DNA-binding affinity for **1** and **2**.

Fluorescence Studies. The fluorescence emission of **1**−**3**, **8**, and **9** were also monitored upon the binding of these systems to DNA. In the case of **1**−**3**, the emission was found to be significantly affected at large *ct*-DNA concentrations. The fluorescence emission spectra of **1** (8.7 μM) in 10 mM phosphate buffer (pH 7.4) are shown in Figure 3. Upon excitation at the isosbestic point, ~415 nm and the successive addition of *ct*-DNA (0−245 μM), the emission intensity of **1** dramatically decreased by ca. 90% at λ_{maxEm} = 510 nm and exhibited a concomitant bathochromic shift of 34 nm. Such fluorescence quenching can be attributed to an efficient photoinduced electron transfer (PET) from the DNA bases to the excited state of the naphthalimide fluorophore. The fluorescence excitation spectra of **1** in the absence and the presence of 245 μM DNA is also shown in Figure 3A, demonstrating the same affect. In comparison, the emission spectra of **2** exhibited a hypochromic effect of ca. 75% (at λ_{maxEm} of 510 nm), accompanied by a bathochromic shift of 19 nm. Upon an increasing concentration of *ct*-DNA (0 → 245 μM), the fluorescence intensity of the emission of **3** at pH 7.4 was quenched by 60%, whereas at pH 6.3, the emission and excitation spectra exhibited a larger hypochromism of 70%. However, these changes were not accompanied by a significant bathochromic shift at the wavelength of λ_{max}. As for the ground-state investigations, the binding of **1** and **2** to *ct*-DNA in competitive media gave rise to similar changes in their fluorescence emission spectra to that in the absence of added NaCl involving significant quenching of emission (ca. 70%) and bathochromic shifts of ca. 28 nm, as shown for **1** in Figure 3B, for a titration with *ct*-DNA in the presence of 160 mM NaCl concentration, clearly showing the high affinity these compounds have for the DNA, even in such a competitive media.

Plots of I/I_0 at 415 nm vs P/D are shown in Figure 4 and demonstrate the dramatic reduction in the emission intensity of both **1** and **2** in comparison to that observed for **3**, on successive addition of *ct*-DNA. This corresponds to an approximately 9-fold and 7-fold decrease in the luminescence intensity of **1** and **2**, respectively, when bound to *ct*-DNA. In comparison, **3** showed a more modest 5-fold decrease at pH 7.4 but when measured at pH 6.3, a 6-fold decrease in the luminescence intensity occurred upon binding to *ct*-DNA.

(19) Carter, M. T.; Rodriguez, M.; Bard, A. J. *J. Am. Chem. Soc.* **1989**, *111*, 8901.

(20) (a) Rogers, J. E.; Weiss, S. J.; Kelly, L. A. *J. Am. Chem. Soc.* **2000**, *122*, 427. (b) Rogers, J. E.; Kelly, L. A. *J. Am. Chem. Soc.* **1999**, *121*, 3854.

(21) Yen, S.-F.; Gabbay, E. J.; Wilson, W. D. *Biochemistry* **1982**, *21*, 2070.

(22) Stevenson, K. A.; Yen, S.-F.; Yang, N.-C.; Boykin, D. W.; Wilson, W. D. *J. Med. Chem.* **1984**, *27*, 1677.

(23) Waring, M. J.; Gonzalez, A.; Jiménez, A.; Vásquez, D. *Nucleic Acids Res.* **1979**, *7*, 217.

(24) Brana, M. F.; Cacho, M.; Garcia, M. A.; de Pascual-Teresa, B.; Ramos, A.; Dominguez, M. T.; Pozuelo, J. M.; Abradelo, C.; Rey-Stolle, M. F.; Yuste, M.; Banez-Coronel, M.; Lacal, J. C. *J. Med. Chem.* **2004**, *47*, 1391.

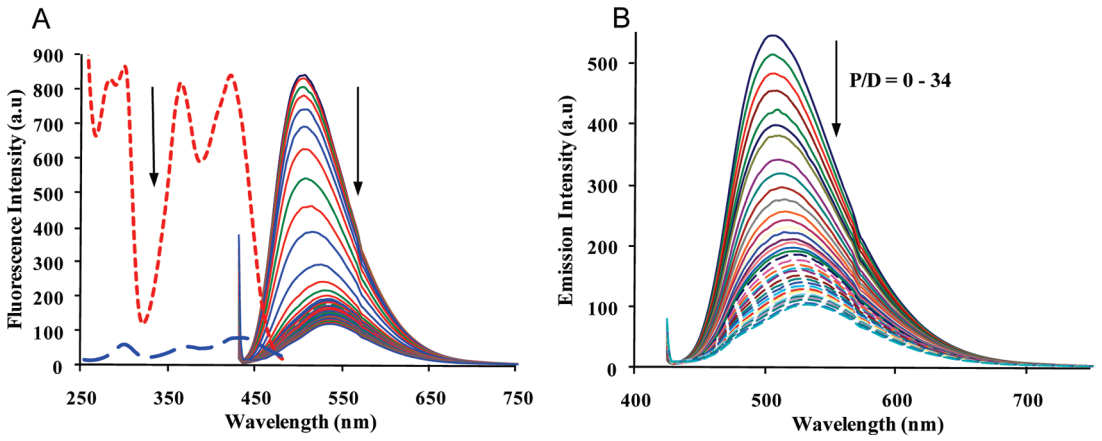

FIGURE 3. (A) Overlaid excitation (λ_{Em} 505 nm) and emission spectra (λ_{Ex} 415 nm) of **1** in 10 mM phosphate buffer (pH 7.4) upon the addition of increasing concentration of *ct*-DNA (0 − 245 μM). (B) Overlaid emission spectra (λ_{Ex} 410 nm) of **1** (8.7 μM, 10 mM phosphate buffer, pH 7.4) in 160 mM NaCl, upon titration with *ct*-DNA.

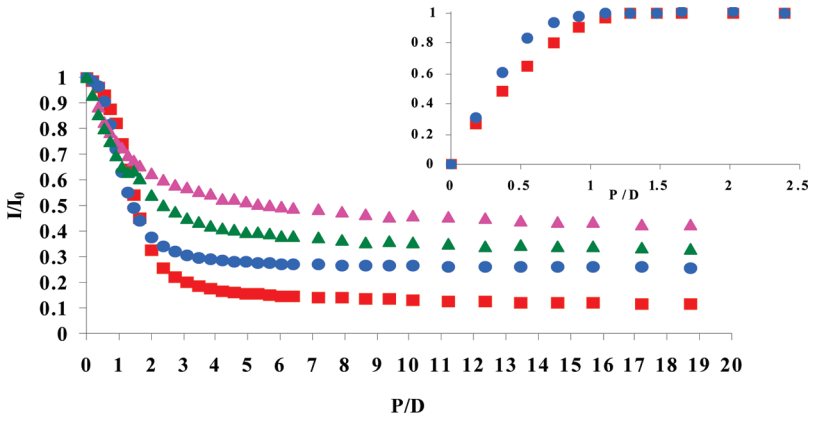

FIGURE 4. Plot of the changes in the emission spectra (λ_{ex} 415 nm) of **1** (red), **2** (blue), and **3** (green) in 10 mM phosphate buffer (pH 7.4) and **3** (pink) in 10 mM coadcylate buffer (pH 6.3) with respect to increasing concentration of *ct*-DNA. Inset: The binding curve for the changes in absorbance at 381 nm for **1** (red) and **2** (blue).

The fluorescence−titration data obtained from the changes in the emission spectra of **1**−**3** in the absence and in the presence of added salt were further used to derive Scatchard plots (see the Supporting Information for **1**−**3**), which were analyzed according to the model of McGhee and von Hippel[25] to determine the K_b values as listed in Table 3. It is clear from the results that these Tröger's base based naphthalimides have a strong binding affinity for DNA with K_b values being determined in the range of 10^6 M^{-1} for **1**−**3**, and as expected, K_b values only slightly decreased when determined in more competitive media. Moreover, the K_b values for **1** and **2** are approximately 14 times larger than that observed for **3** at physiological pH, presumably because of the binding contribution of their protonated amino side chain as discussed above. As had been anticipated, the K_b value for **3** determined at pH 6.0 was larger than that determined at pH 7.0, which supports this argument. To further examine the strength of DNA binding in competitive media the changes in the luminescence intensity of **1** and **2** when fully bound to *ct*-DNA was monitored, upon the addition of an increasing amount of a 2 M NaCl solution. For both **1** and **2**, the addition of an increasing concentration of NaCl (see example of a back-titration in Supporting Information) did not result in any significant increase in the luminescence intensity indicating that indeed both **1** and **2** bind strongly to DNA and also signify that such a DNA-binding processes is irreversible.

TABLE 3. Binding Constants Determined from the Emission Spectra for 1−3 in 10 mM Phosphate Buffer at pH 7.4 and in the Presence of Competitive Media and 3* in 10 mM Codaylate Buffer at pH 6.0

K_b ($\times 10^6$ M^{-1})	1	2	3	3*
0 mM NaCl	1.75 (±0.04)	2.56 (±0.09)	0.18 (±0.012)	0.80 (±0.08)
50 mM NaCl	1.03 (±0.05)	0.96 (±0.03)		
160 mM NaCl	0.72 (±0.03)	0.1 (±0.02)		

We also investigated the binding affinity of **7** and **8** under identical conditions as descried above. The emission spectra of **7** (8.7 μM, 10 mM phosphate buffer, pH 7.4) in the absence and presence of *ct*-DNA (P/D = 0−34) upon excitation at 433 nm are shown in Figure S11A (right, see the Supporting Information). Upon the titration with *ct*-DNA (0 → 245 μM), the emission spectra of **7** was found to decrease by 44% (at λ_{em} = 548 nm); however, unlike that seen for **1**, these changes were also accompanied by a hypsochromic shift of ca. 12 nm.[26] Analysis of these changes showed that the emission intensity of **7** was reduced by ca. 4-fold upon binding to *ct*-DNA, while the Tröger's base **1** (Figure 3A)

(25) McGhee, J. D.; von Hippel, P. H. *J. Mol. Biol.* **1974**, *86*, 469.

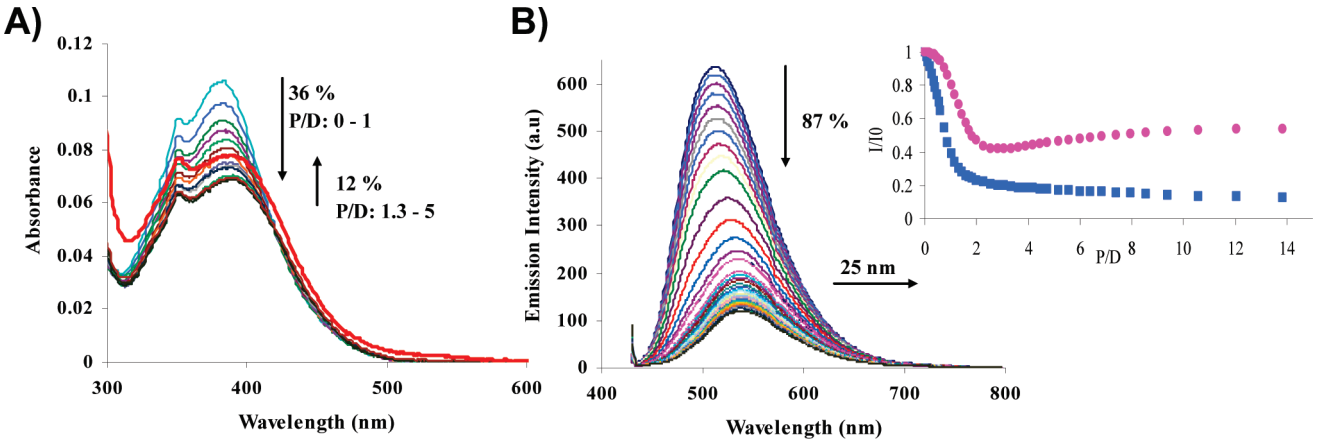

FIGURE 5. (A) Changes in the absorption spectra of **1** (8.2 μM) upon the successive addition of poly(dG-dC) (0.5 mM). (B) Corresponding changes in the emission spectra. Inset: Plot of the changes in the emission spectra of **1** in the presence of poly(dG-dC) (■) (λ_{ex} 417 nm) and poly(dA-dT) (●) (λ_{ex} 415 nm).

gave rise to a significant 9-fold reduction in emission. Also shown in Figure S11A (left, see the Supporting Information) are the changes observed in the excitation spectra of **7** upon binding to DNA, being significantly different than that observed for **1** in Figure 3A. In contrast to these results then, upon titration of **8** with DNA (excitation at 433 nm), only minor changes were observed where the emission spectra exhibited the appearance of an isoemissive point at 548 nm, accompanied by a hypsochromic shift of 12 nm. When **8** was excited at 361 nm, the changes observed were a hypochromism of 36% accompanied by a hypsochromic shift of 17 nm, whereas significant hyperchromism of 45% with a concomitant hypsochromic shift of 16 nm was observed in the emission spectrum when **8** was excited at the isosbestic point 473 nm. Such changes were not observed in the emission spectra of **7** (λ_{Em} at 433 nm) upon binding to *ct*-DNA, clearly demonstrating that the excited state of these two precursors were differently affected upon biding to DNA.[26] Analysis of the emission data for **7** permitted a determination of the binding constant K_b based on fitting the changes using the McGhee and von Hippel model, as 0.98 ($\pm$0.03) $\times$ 10^6 M^{-1}. However, the changes observed for **8** were too small, Figure S11B (Supporting Information), to allow for an accurate binding constant determination upon excitation of the ICT band. Nevertheless, the changes observed upon excitation at the isosbestic point at 361 nm enabled us to determine the K_b for **8**, as 0.20 ($\pm$0.02) $\times$ 10^6 M^{-1}, while excitation at 473 nm gave K_b = 0.23 ($\pm$0.04) $\times$ 10^6 M^{-1}. In comparison to that observed for **1** and **2**, these binding constants are significantly smaller, being ca. 2 times less for **7** than that observed for **1** and nearly 10-fold smaller for **8** than seen for **2**. Hence, the overall results clearly demonstrated that (i) the emission of **1** and **2** is significantly more sensitive to the binding of DNA than that of **7** and **8** and (ii) the Tröger's bases give rise to stronger binding.

(26) Compound **7** was also excited at the isosbestic point 473 nm. This gave rise to an increased by 15% (at λ_{em} = 530 nm) and showed the appearance of an isoemissive point at 550 nm upon binding to *ct*-DNA. These latter changes were also accompanied by a 10 nm hypsochromic shift. When **8** was excited at 361 nm, a hypochromism of 36% was observed which was accompanied by a hypsochromic shift of 17 nm. Significant hyperchromism of 45%, with a concomitant hypsochromic shift of 16 nm. was also observed in the emission spectrum of **8** when excited at 473 nm, the isosbestic point.

Binding of 1 and 2 to Polynucleotides. In order to investigate the sequence specificity of these naphthalimide Tröger's bases, the binding interactions of compounds **1** and **2** with the two polynucleotides, poly(dA-dT) and poly(dG-dC), were evaluated in a similar manner to that with *ct*-DNA above. For both, the changes in the absorption spectra were similar to those observed in the case of *ct*-DNA; i.e., hypochromism and a red shift were seen in the ICT absorption band followed by an increase in the absorption band at higher P/D ratios, as demonstrated in Figure 5A for **1**. The appearance of an isosbestic point was also observed during these titrations. The binding constants for the interaction of **1** with poly(dG-dC) and poly(dA-dT) were determined by fitting the changes in the absorption spectra to the Brad model in a similar manner to that done for *ct*-DNA above. For these changes, K_b values of 2.42 ($\pm$0.2) $\times$ 10^6 M^{-1} and 2.83 ($\pm$0.2) $\times$ 10^6 M^{-1} were determined for poly(dG-dC) and poly(dA-dT), suggesting that **1** did not bind to DNA in a sequence specific manner.

Changes in the emission spectra of **1** involved an overall red shift in the fluorescence where an initial quenching followed by an emission enhancement with increasing P/D ratios was observed. However, these changes were dependent on the polynucleotides used, as demonstrated for poly(dG-dC) in Figure 5B, which gave rise to ca. 87% quenching, while poly(dA-dT) gave rise to ca. 57% quenching, which was then followed by slight enhancement at higher P/D ratios. These effects are shown in Figure 5B as an inset, which demonstrates the decrease in the emission of **1** upon interaction with poly(dG-dC), reaching a plateau at a P/D ratio of ca. 14, whereas upon interaction with poly(dA-dT), the emission decreased until a P/D of about 3 and thereafter increased, leveling off at a P/D of about 13. These changes (which were found to be fully reproducible) indicated that two processes were occurring on binding to poly(dA-dT) the first of them probably involving the external binding of the molecule to the DNA surface (electrostatic interactions), while the second interaction could involve the binding of **1** in the grooves of the DNA. A binding constant K_b of 1.33 $\times$ 10^6 M^{-1}, was determined for the binding of **1** ith poly(dG-dC), by fitting the changes in the emission spectra to the method of McGhee and von Hippel, a result which again demonstrates

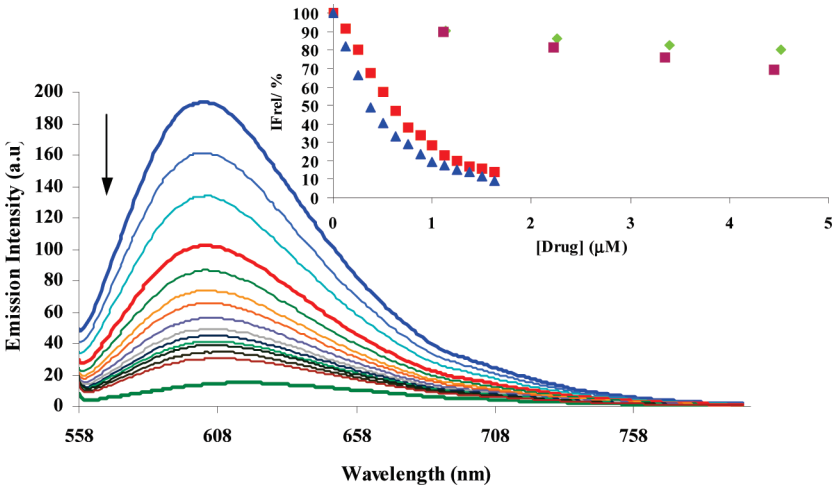

FIGURE 6. Emission spectra of EtBr (1.25 μM) when free (green line) and bound to *ct*-DNA (2.5 μM, blue line) in 10 mM phosphate buffer upon the titration of **1** (0→1.8 μM). Inset: Fluorescence decrease of EtBr induced by the competitive binding of **1** (▲, blue), **2** (■, red), **4** (■, purple), and **5** (♦, green) to *ct*-DNA.

a very high affinity of **1** for this DNA structure. However, a binding constant for the interactions with poly(dA-dT) could not be determined accurately from the emission data.

Similarly, the binding of **2** also gave rise to large changes in both the absorption and the emission spectra upon interaction with these homopolymers. For the ground-state interaction, the degree of hypochromism observed upon the successive addition of poly(dG-dC) was approximately 43%, while it was ca. 36% for poly(dA-dT). These changes reached a plateau at a P/D of approximately 2. Unfortunately, fitting of the initial absorbance data to the Bard model gave rise to the same binding constant for the interaction of **2** with each of the polynucleotides, with a K_b of 2.6×10^6 M^{-1}. As seen above, the overall changes observed in the emission spectra of **2** upon binding to poly(dA-dT) and poly(dG-dC) were similar to that seen for **1** and gave a K_b value of 3.5×10^6 M^{-1} for the binding of **2** to poly(dG-dC). This value is nearly a three-times greater binding constant than the K_b observed for **1**, indicating that **2** has a significant greater affinity for poly(dG-dC) than **1**. Again K_b could not be determined for the interaction with poly(dA-dT) from the changes in the emission spectra. As a means of monitoring the binding preference of **2** with either AT- or GC-rich sequences, a competitive binding assay were also carried out, which involved adding fixed aliquots of poly(dA-dT) to a solution mixture of **2**/poly(dG-dC) at a P/D of about 2 and monitoring any reverse changes in fluorescence emission. As before, the emission of **2** bound to poly(dG-dC) was significantly quenched. However, the subsequent addition of poly(dA-dT) resulted in the progressive restoring of the luminescence intensity up to a P/D = 16. At this stage, fixed aliquots of poly(dG-dC) were added. However, the emission was seen to only slightly decrease, indicating that **2** was more tightly bound to poly(dA-dT) than to poly(dG-dC). However, these are not conclusive results regarding sequence specificity; they seem to indicate that the Tröger's bases could bind more strongly to poly(dA-dT) over poly(dG-dC).

Ethidium Bromide (EtBr) Displacement Assays Using 1−2 and 7−8. With the view of further quantifying the binding affinity of the Tröger's bases **1** and **2** in comparison to their precursors **7** and **8**, we carried out ethidium bromide displacement assay,[26] in 10 mM phosphate buffer (pH 7.4) according to the procedures developed by Cain et al. and Boger et al., respectively.[27,28] Here, the changes in the emission spectra of EtBr bound to DNA were then monitored upon the successive additions of 2 μL aliquots of either **1** or **2**. The emission spectrum for the titration of EtBr bound to *ct*-DNA with **1** is shown in Figure 6, which upon titration with **1** caused the emission intensity of EtBr/*ct*-DNA at λ_{max} = 600 nm to decrease dramatically, indicating that **1** is highly capable of substituting for EtBr bound to DNA. In comparison, the precursors **7** and **8** only gave rise to minor changes in the emission spectrum of the EtBr, indicating that these structures did not display the dye in as dramatic a manner as the Tröger's bases. This is clear from the plots of the relative decrease in intensity (IFrel/%) of EtBr/*ct*-DNA against the concentration of added **1**−**2** and **7**−**8**, which are shown as an inset in Figure 6. Analysis of the emission data from each of these titrations allowed for a determination of their respective C_{50} values and corresponding apparent binding constants, K_{app}. The results are summarized in Table 4, and it is clear from these results that all are capable of displacing EtBr effectively from bound *ct*-DNA, which gives rise to a quenching of the emission of EtBr; however, the C_{50} values for which such displacement is achieved are significantly smaller for both **1** and **2** in comparison to that of their precursors **4** and **5**, highlighting their greater DNA binding affinity. The sequence specificity of these compounds was also evaluated in phosphate buffer using poly(dG-dC) and poly(dA-dT). The relevant C_{50} and K_{app} values were summarized in Table 4. According to these results, both **1** and **2** displace EtBr from poly(dG-dC) and poly(dA-dT) at nearly the same C_{50} values. On the other hand, **7** and **8** exhibit sequence specificity by displacing ethidium bromide from poly(dA-dT) at C_{50} values that were two times lower than those for poly(dG-dC). The results from these EtBr displacement assays with *ct*-DNA were in good agreement with the results from the ground- and excited-state investigations, and the trends in the K_b

(27) (a) Boger, D. L.; Fink, B. E.; Hedrick, M. P. *J. Am. Chem. Soc.* **2000**, *122*, 6382. (b) LePecq, J.-B.; Paoletti, C. *J. Mol. Biol.* **1967**, *27*, 87.

(28) (a) Tse, W. C.; Boger, D. L. *Acc. Chem. Res.* **2004**, *37*, 61. (b) Cain, B. F.; Baguley, B. C.; Denny, W. A. *J. Med. Chem.* **1978**, *19*, 1101.

TABLE 4. C_{50} Values and Corresponding Binding Constants K_{app} for the Tröger's Bases 1 and 2, as Well as the Precursors 7 and 8, Determined from an EtBr Displacement Assay (All in 10 mM Phosphate Buffer at pH 7.4) Using *ct*-DNA and the Homopolymers Poly(dG-dC) and Poly(dA-dT)

	1	2	7	8
ct-DNA				
C_{50} (μM)	0.38	0.63	10	25
K_{app} ($\times 10^7$ M^{-1})	3.5	2.4	0.15	0.05
poly(dG-dC)				
C_{50} (μM)	1.0	0.85	7.75	25
K_{app} ($\times 10^7$ M^{-1})	0.089	0.11	0.012	0.0039
poly(dA-dT)				
C_{50} (μM)	0.75	0.60	12	44
K_{app} ($\times 10^7$ M^{-1})	2.0	2.4	0.12	0.034

values with *ct*-DNA are in the same order as seen from both the absorbance and emission data above. Unfortunately, the sequence specificity of **1** and **2** was not accurately determined for the same reasons as discussed above. However, the results showed that both **1** and **2** exhibit a significantly stronger binding interaction with the polynucleotides in comparison to **7** and **8**.

Thermal Denaturation Studies of 1−3 and 7−9. To further evaluate the DNA binding affinity of **1** and **2**, thermal denaturation (T_m) studies were also conducted. For the melting temperature measurements, the T_m of *ct*-DNA (150 μM) alone and in the presence of **1** and **2** (P/D ratio of 10) were carried out in 10 mM phosphate buffer (pH 7.4). From these studies, both **1** and **2** stabilized the *ct*-DNA structure to a large extent, as is displayed in the thermal displacement curves of *ct*-DNA shown in Figure S12 (see the Supporting Information), whereby **1** and **2** gave rise to an increase of ca. $\Delta T_m > 15$ °C (see the table inset in Figure 12 (Supporting Information). In fact, such an increase in T_m was found to be significantly larger in comparison to that of **7** and **8**, which only gave rise to a ΔT_m of 5 °C, confirming that the Tröger's base moiety has an influence on such enhanced DNA binding affinity. The ability of **1** and **2** to stabilize poly(dAdT) toward thermal denaturation was also analyzed, and it was found that both gave rise to a substantial increase of ca. >20 °C in the melting temperature of poly-(dA-dT) (see the Supporting Information), clearly demonstrating the advantages of the incorporation of the diazocine ring into these structure and, hence, also clearly reflecting the advantages of the use of C_2 plane of symmetry of the molecules.

Conclusion

In this paper, we have shown that the synthesis of the novel fluorescent supramolecular cleft-like 1,8-naphthalimide-based Tröger's bases **1−3** was achieved in reasonable yields after optimization of reaction conditions, and their photophysical characteristics were determined in a range of solvents of varying polarity and hydrogen-bonding capability and compared to their 4-amino-1,8-naphthlaimide precursors **7−9** using both ground-state and excited-state spectroscopy. Our results showed that by the incorporation of the Tröger's base moiety into the skeleton of the 4-amino-1,8-naphtalimides, such supermolecules exhibited an ICT excited state which was indeed solvatochromic. The absorbance spectral changes obtained with respect to pH, allowed for a determination of the pK_a values of their "terminus" alkylamine substituents. It was found that **1** and **2** having pK_a values of 8.7 and 8.2, respectively, would indeed be protonated at physiological pH. However, **3** with a pK_a value of 6.0 would not be expected to give rise to significant electrostatic interactions with DNA. Indeed, by using UV/vis absorption and fluorescence titrations, this would found to be the case with both **1** and **2** showing significantly stronger DNA binding affinity even in the presence of competitive media (50 mM or 160 mM NaCl), whereby K_b values in the range of 10^6 M^{-1} were determined for **1** and **2**. The DNA binding affinity of **1** and **2** was further examined by carrying out T_m experiments whereby there was a significant stabilization of the DNA structure by **1** and **2** and also from the ethidium bromide displacement assays, and it was found that the results were in good agreement with those obtained from the ground- and excited-state investigations by exhibiting similar trends in DNA binding affinity, with **1** and **2** being significantly more competitive with EtBr toward binding with DNA that that of **3** and **4** .

In summary, the results from this investigation demonstrate that naphthalimide-based Tröger's bases **1−3** are very promising supramolecular binders for DNA, where the presence of the diazocine ring gives rise to a large enhancement in the affinity of these compounds to *ct*-DNA and for the homopolymers poly(dA-dT) and poly(dG-dC). In addition to this work, we have carried out a detailed biological investigation of the Tröger's bases **1−3** in various cancer cell lines and shown that all three are taken up by cancer cells and that they localize within the nucleus, giving rise to apoptotic cell death.[9a] This part of our investigation will be published at a later date as a full account. We are currently developing other analogues of **1−3** as DNA targeting supramolecular binders by modifying the aromatic ring as well as incorporating other structures at the imide sites.

Experimental Section

General Experimental Procedure for Compounds 4−6. The appropriate dialkylaminoethylamine (1.4 equiv) was added to a solution of 4-nitro-1,8-naphthalic anhydride (1 equiv) in anhydrous toluene. The reaction mixture was stirred at reflux (120 °C) for 48 h under an argon atmosphere and in the presence of molecular sieves. The reaction mixture was then filtered while hot through Celite, washing several times with toluene. The filtrate and washings were removed under reduced pressure, and the residue was dissolved in CH_2Cl_2. The organic solution was washed twice with satd $NaHCO_3$, twice with H_2O, and once with brine. The organic layer was dried over $MgSO_4$ and evaporated under reduced pressure to dryness. The crude product was then purified by recrystallization using either EtOH or MeOH.

***N*-[1-Dimethylaminoethyl]-4-nitro-1,8-naphthalimide (4)[20].** Compound **4** was synthesized by reacting *N,N*-dimethylethylenediamine (1.50 g, 1.86 mL, 17.3 mmol, 1.4 equiv) with 4-nitro-1,8-naphthalic anhydride (3.0 g, 12 mmol, 1 equiv) and Et_3N (2.5 g, 3.56 mL, 24.6 mmol, 2 equiv) in anhydrous toluene (200 mL) to yield the product as a shiny brown solid (2.83 g, 91%) after a recrystallization from EtOH: mp 106−108 °C (lit.[20] mp 106−109 °C); HRMS 314.1141 ($[M + H]^+$, $C_{16}H_{16}N_3O_4$ requires 314.1129); NMR δ_H (400 MHz, $CDCl_3$), 8.80 (1H, d, J = 8.5 Hz, Ar-H7), 8.71 (1H, d, J = 7.0 Hz, Ar-H5), 8.67 (1H, d, J = 8.0 Hz, Ar-H2), 8.39 (1H, d, J = 8.0 Hz, Ar-H3), 7.97 (1H, dd, J = 8.0 and 7.5 Hz, Ar-H6), 4.33 (2H, t, J = 7.0 Hz, $NCH_2CH_2N(CH_3)_2$), 2.67 (2H, t, J = 7.0 Hz, $NCH_2CH_2N(CH_3)_2$), 2.35 (6H, s, $N(CH_3)_2$); NMR δ_C (100 MHz, $CDCl_3$), 162.9, 162.0,

149.0, 132.0, 129.4, 129.3, 128.8, 128.6, 126.4, 123.4, 123.1, 122.5, 56.4, 45.3, 38.0; MS m/z 314 $(M + H)^+$.

***N*-[1-Methylpyprazinoethyl]-4-nitro-1,8-naphthalimide (5).** Compound **5** was synthesized by reacting 1-(2-aminoethyl)-4-methylpiperazine (2.47 g, 2.58 mL, 17.2 mmol, 1.4 equiv) with 4-nitro-1,8-naphthalic anhydride (3.0 g, 12.3 mmol, 1 equiv) and Et_3N (2.5 g, 3.56 mL, 24.6 mmol, 2 equiv) in anhydrous toluene (200 mL), to yield the product as a brown solid (3.50 g, 77%) after a recrystallization from MeOH: mp 109−111 °C; HRMS 369.1554 ($[M + H]^+$, $C_{19}H_{21}N_4O_4$ requires 369.1563); NMR δ_H (400 MHz, $CDCl_3$), 8.85 (1H, d, J = 9.0 Hz, Ar-H7), 8.74 (1H, d, J = 7.5 Hz, Ar-H5), 8.70 (1H, d, J = 8.0 Hz, Ar-H2), 8.42 (1H, d, J = 8.0 Hz, Ar-H3), 8.00 (1H, t, J = 8.0 Hz, Ar-H6), 4.36 (2H, t, J = 7.0 Hz, $NCH_2CH_2N(CH_2CH_2)_2NCH_3$), 2.73 (2H, t, J = 7.0 Hz, $NCH_2CH_2N(CH_2CH_2)_2NCH_3$), 2.65(4H, s, $NCH_2CH_2N(CH_2CH_2)_2NCH_3$), 2.44 (4H, br s, $NCH_2CH_2N(CH_2CH_2)_2NCH_3$), 2.28 (3H, s, $NCH_2CH_2N(CH_2CH_2)_2NCH_3$); NMR δ_C (100 MHz, $CDCl_3$) 162.7, 161.9, 149.0, 131.8, 129.4, 129.2, 128.7, 128.5, 126.4,123.4, 123.1, 122.4, 54.9, 54.6, 52.7, 45.5, 45.5, 37.3; MS m/z 369 $(M + H)^+$; IR ν_{max} (neat sample)/cm^{-1} 3078, 2928, 2793, 2757, 1655, 1522,1339, 824, 761.

***N*-(1-Morpholinoethyl)-4-nitro-1,8-naphthalimide (6).** Compound **6** was synthesized by reacting 4-(2-aminoethyl)morpholine (1.60 g, 1.62 mL, 12.3 mmol, 1 equiv) with 4-nitro-1,8-naphthalic anhydride (3.0 g, 12.3 mmol, 1 equiv) in toluene (30 mL) to yield the product as a brown solid (3.17 g, 74%) after a recrystallization from EtOH: mp 115−117 °C; HRMS 355.3663 ($[M + H]^+$, $C_{18}H_{18}N_3O_5$ requires 355.3563); NMR δ_H (400 MHz, $CDCl_3$) 8.84 (1H, d, J = 8.5 Hz, Ar-H7), 8.73 (1H, d, J = 7.5 Hz, Ar-H5), 8.69 (1H, d, J = 8.0 Hz, Ar-H2), 8.41 (1H, d, J = 8.0 Hz, Ar-H3), 8.00 (1H, t, J = 8.0 Hz, Ar-H6), 4.37 (2H, t, J = 7.0 Hz, $NCH_2CH_2N(CH_2CH_2)_2O$), 3.69 (4H, t, J = 4.5 Hz, $NCH_2CH_2N(CH_2CH_2)_2O$), 2.75 (2H, t, J = 4.5 Hz, $NCH_2CH_2N(CH_2CH_2)_2O$), 2.63 (4H, br s, $NCH_2CH_2N(CH_2CH_2)_2O$); NMR δ_C (100 MHz, $CDCl_3$), 162.9, 162.0, 149.1, 132.0, 129.5, 129.4, 128.9, 128.4, 126.4, 123.5, 123.2, 122.5, 66.4, 55.5, 53.3, 36.9; MS m/z 355 $(M + H)^+$; IR ν_{max} (neat sample)/cm^{-1} 3078, 2950, 2855, 1656, 1523, 1339, 1117, 839, 787.

General Experimental Procedure for Compounds 7−9. The reduction reaction of the relevant 4-nitro-1,8-naphthalimide (1 equiv) in MeOH was carried out using a Parr hydrogen shaker apparatus at 3 atm of pressure in the presence of 10% Pd/C catalyst (0.2 equiv) until no more hydrogen gas was consumed. The reaction mixture was filtered through Celite and washed with MeOH. The filtrate and washings were evaporated under reduced pressure and further dried under vacuum.

***N*-(1-Dimethylaminoethyl)-4-amino-1,8-naphthalimide (7)[19].** Compound **7** was synthesized using **4** (1.80 g, 5.7 mmol, 1 equiv) and was yielded as an orange solid (1.57 g, 98%): mp 184−185 °C (lit.[19] mp 184−185 °C); HRMS 284.1399 ($[M + H]^+$, $C_{16}H_{18}N_3O_2$ requires 284.1388); NMR δ_H (400 MHz, $(CD_3)_2SO$), 8.60 (1H, d, J = 8.5 Hz, Ar-H7), 8.41 (1H, d, J = 7.0 Hz, Ar-H2), 8.18 (1H, d, J = 8.0 Hz, Ar-H5), 7.64 (1H, dd, J = 7.5 and 8.5 Hz, Ar-H6), 7.46 (2H, br s, NH_2), 6.83 (1H, d, J = 8.5 Hz, Ar-H3), 4.11 (2H, t, J = 7.0 Hz, $NCH_2CH_2N(CH_3)_2$), 2.51 (2H, t, J = 7.0 Hz, $NCH_2CH_2N(CH_3)_2$), 2.08 (6H, s, $N(CH_3)_2$); NMR δ_C (100 MHz, $(CD_3)_2SO$), 163.7, 162.8, 152.7, 133.9, 131.0, 129.6, 129.3, 123.9, 121.7, 119.3, 108.1, 107.4, 56.6, 45.3, 37.0; MS m/z 284 $(M + H)^+$.

***N*-(1-Methylpyprazinoethyl)-4-amino-1,8-naphthalimide (8).** Compound **8** was synthesized using **5** (1.0 g, 2.7 mmol, 1 equiv) and was obtained as an orange solid (900 mg, 98%): mp 182−183 °C; HRMS 361.1829 ($[M + Na]^+$, $C_{19}H_{22}N_4O_2Na$ requires 361.1821); NMR δ_H (400 MHz, $(CD_3)_2SO$), 8.62 (1H, d, J = 8.5 Hz, Ar-H7), 8.41 (1H, d, J = 7.0 Hz, Ar-H2), 8.18 (1H, d, J = 8.5 Hz, Ar-H5), 7.65 (1H, t, J = 8.0 Hz, Ar-H6), 7.46 (2H, br s, NH_2), 6.84 (1H, d, J = 8.5 Hz, Ar-H3), 4.12 (2H, t, J = 7.0 Hz, $NCH_2CH_2N(CH_2CH_2)_2NCH_3$), 3.25 (2H, t, J = 7.0 Hz, $NCH_2CH_2N(CH_2CH_2)_2NCH_3$), 2.45 (4H, br s, $NCH_2CH_2N(CH_2CH_2)_2NCH_3$), 2.29 (4H, br s, $NCH_2CH_2N(CH_2CH_2)_2NCH_3$), 2.13 (3H, s, $NCH_2CH_2N(CH_2CH_2)_2NCH_3$); NMR δ_C (100 MHz, $(CD_3)_2SO$), 163.7, 162.8, 152.7, 133.9, 131.0, 129.6, 129.3, 123.9, 121.7, 119.3, 108.1, 107.4, 55.3, 54.6, 52.7, 45.6, 36.6; MS m/z 339 $(M + H)^+$; IR ν_{max} (neat sample)/cm^{-1} 3211, 2928, 2882, 2807, 2695, 1678, 1641, 1574, 816, 755.

***N*-(1-Morpholinoethyl)-4-amino-1,8-naphthalimide (9).** Compound **9** was synthesized using **6** (1.0 g, 2.7 mmol, 1 equiv) and was obtained as a yellow solid (800 mg, 87%): mp 175−177 °C; HRMS 348.3829 ($[M + Na]^+$, $C_{18}H_{19}N_3O_3Na$ requires 348.3828); NMR δ_H (400 MHz, $(CD_3)_2SO$), 8.60 (1H, d, J = 8.0 Hz, Ar-H7), 8.41 (1H, d, J = 7.0 Hz, Ar-H2), 8.18 (1H, d, J = 8.5 Hz, Ar-H5), 7.64 (1H, t, J = 8.0 Hz, Ar-H6), 7.46 (2H, br s, NH_2), 6.83 (1H, d, J = 8.5 Hz, Ar-H3), 4.13 (2H, t, J = 7.0 Hz, $NCH_2CH_2N(CH_2CH_2)_2O$), 3.54 (4H, br s, $NCH_2CH_2N(CH_2CH_2)_2O$), 2.54 (2H, br s, $NCH_2CH_2N(CH_2CH_2)_2O$), 2.45 (4H, br s, $NCH_2CH_2N(CH_2CH_2)O$); NMR δ_C (100 MHz, $(CD_3)_2SO$), 163.7, 162.8, 152.7, 133.9, 131.0, 129.6, 129.3, 123.9, 121.7, 119.3, 108.1, 107.4, 66.2, 55.8, 53.4, 36.4; MS m/z 348 $(M + H)^+$; IR ν_{max} (neat sample)/cm^{-1} 3253, 2964, 2919, 2861, 2813, 1638, 1572, 863, 774.

General Procedure for the Synthesis of 1−3. A mixture of the relevant 4-amino-1,8-naphthalimide (1 equiv) and paraformaldehyde (1.5 equiv) in neat TFA was stirred at room temperature for 12 h under an argon atmosphere. The reaction was then brought to pH 9/12 (depending on pK_a value of the molecule) by the slow addition of aqueous NaOH (6 M). The aqueous solution was extracted three times with CH_2Cl_2. The organic extracts were combined, and the solvent was removed under reduced pressure. The crude product was purified by recrystallization from EtOH and dried under vacuum.

Bis[*N*-(1-Dimethylaminoethyl)]-9,18-methano-1,8-naphthalimido[*b,f*][1,5]diazocine (1). Compound **1** was synthesized by reacting **7** (200 mg, 0.71 mmol, 1 equiv) with paraformaldehyde (32.5 mg, 0.03 mL, 1.1 mmol, 1.5 equiv) in TFA (3.5 mL) to yield the product as an orange solid (260 mg, 61%) after recrystallization from EtOH: mp 231−233 °C; HRMS 603.2740 ($[M + H]^+$, $C_{35}H_{35}N_6O_4$ requires 603.2720); NMR δ_H (400 MHz, $CDCl_3$), 8.69(2H, d, J = 8.0 Hz, Ar-H7, Ar-H7′), 8.60 (2H, d, J = 7.5 Hz, Ar-H5, Ar-H5′), 8.07 (2H, s, Ar-H2, Ar-H2′), 7.87 (2H, t, J = 8.0 Hz, Ar-H6, Ar-H6′), 5.12 (2H, d, J = 17.0 Hz, Ar-CH_2N), 4.67 (2H, s, NCH_2N), 4.59 (2H, d, J = 17.0 Hz, Ar-CH_2N), 4.29 (4H, t, J = 6.5 Hz, $NCH_2CH_2N(CH_3)_2$), 2.64 (4H, t, J = 6.5 Hz, $NCH_2CH_2N(CH_3)_2$), 2.30 (12H, s, $N(CH_3)_2$); NMR δ_C (100 MHz, $CDCl_3$), 163.7, 163.1, 148.6, 130.5, 130.0, 128.3, 127.8, 126.8, 126.7, 124.7, 122.6, 118.4, 66.6, 56.6, 56.4, 45.2, 37.5; MS m/z 603 $(M + H)^+$; IR ν_{max} (neat sample)/cm^{-1} 2955, 2859, 2819, 2769, 1652, 1595, 787. Anal. Calcd for $C_{35}H_{34}N_6O_4$: C, 69.75; H, 5.69; N, 13.94. Found: C, 69.53; H, 5.62; N, 13.56.

Bis[*N*-(1-Methylpyprazinoethyl)]-9,18,-methano-1,8-naphthalimido[*b,f*][1,5]diazocine (2). Compound **2** was synthesized by reacting **8** (200 mg, 0.059 mmol, 1 equiv) with paraformaldehyde (21.6 mg, 0.02 mL, 0.086 mmol, 1.5 equiv) in TFA (3 mL) to yield the product as a yellow solid (210 mg, 50%) after recrystallization from EtOH: mp 225−227 °C; HRMS 713.3580 ($[M + H]^+$, $C_{41}H_{45}N_8O_4$ requires 713.3564); NMR δ_H (400 MHz, $CDCl_3$), 8.62 (2H, d, J = 8.5 Hz, Ar-H7, Ar-H7′), 8.51 (2H, d, J = 7.0 Hz, Ar-H5, Ar-H5′), 8.02 (2H, s, Ar-H2, Ar-H2′), 7.81 (2H, t, J = 8.0 Hz, Ar-H6, Ar-H6′), 5.10 (2H, d, J = 17.0 Hz, Ar-CH_2N), 4.65 (2H, s, NCH_2N), 4.53 (2H, d, J = 17.0 Hz, Ar-CH_2N), 4.23 (4H, t, J = 6.5 Hz, $NCH_2CH_2N(CH_2)_4CH_3$), 2.60 (4H, t, J = 6.5 Hz, $NCH_2CH_2N(CH_2)_4CH_3$), 2.43 (8H, br s, $NCH_2CH_2N(CH_2)_4CH_3$), 2.39 (8H, br s, $NCH_2CH_2N(CH_2)_4CH_3$), 2.23 (6H, s, NCH_3); NMR δ_C (100 MHz, $CDCl_3$), 163.5, 162.9, 148.5, 130.4, 129.8, 128.2, 127.7, 126.7, 126.6, 124.7, 122.5, 118.3, 66.5, 56.5, 55.1, 54.5, 52.6, 45.4, 3 6.8; MS m/z

713 $(M + H)^+$; IR ν_{max} (neat sample)/cm^{-1} 2936, 2795, 1650, 1595, 783. Anal. Calcd for $C_{41}H_{44}N_8O_4$: C, 69.08; H, 6.22; N, 15.72. Found: C, 68.69; H, 6.10; N, 15.71.

Bis[*N*-(1-Morpholinoethyl)]-9,18-methano-1,8-naphthalimido-[*b*,*f*][1,5]diazocine (3). Compound **3** was synthesized by reacting **9** (200 mg, 0.060 mmol, 1 equiv) with paraformaldehyde (27.0 mg, 0.025 mL, 0.092 mmol, 1.5 equiv) in TFA (3 mL) to yield the product as a yellow solid (205 mg, 49%) after a recrystallization from EtOH: mp 231−232 °C; HRMS 687.7180 ($[M + H]^+$, $C_{39}H_{39}N_6O_6$ requires 687.7164); NMR δ_H (400 MHz, $CDCl_3$), 8.70 (2H, d, J = 8.5 Hz, Ar-H7, Ar-H7′), 8.60 (2H, d, J = 7.0 Hz, Ar-H5, Ar-H5′), 8.10 (2H, s, Ar-H2, Ar-H2′), 7.88 (2H, t, J = 8.0 Hz, Ar-H6, Ar-H6′), 5.16 (2H, d, J = 19.5 Hz, Ar-CH_2N), 4.69 (2H, s, NCH_2N), 4.60 (2H, d, J = 17.0 Hz, Ar-CH_2N), 4.30 (4H, br s, $NCH_2CH_2N(CH_2CH_2)_2O$), 3.66 (8H, br s, $NCH_2CH_2N(CH_2CH_2)_2O$), 2.71 (4H, br s, $NCH_2CH_2N(CH_2CH_2)_2O$), 2.61 (8H, br s, $NCH_2CH_2N(CH_2CH_2)_2O$); NMR δ_C (100 MHz, $CDCl_3$), 163.7, 163.1, 148.7, 130.5, 130.0, 128.3, 127.8, 126.8, 126.7, 124.8, 122.6, 118.3, 66.5, 66.2, 56.6, 55.5, 53.1; MS m/z 686 $(M + H)^+$; IR ν_{max} (neat sample)/cm^{-1} 2955, 2863, 2754, 1592, 1112, 783. Anal. Calcd for $C_{39}H_{38}N_6O_6$: C, 68.21; H, 5.58; N, 12.24. Found: C, 67.92; H, 5.26; N, 12.02.

Acknowledgment. We thank the Science Foundation Ireland (SFI RFP 2008 grant), Enterprise Ireland, IRCSET (postgraduate fellowship), Higher Education Authority (HEA-PRTLI Cycle 3 and Cycle 4 grants), CSCB, and TCD for financial support.

Supporting Information Available: General experimental description, synthesis, and characterization of all intermediates; ^1H and ^{13}C NMRs spectra of all intermediates and final products; various figures and tables (see text for reference). This material is available free of charge via the Internet at http://pubs.acs.org.